Evaluation of Intravascular Ultrasound Catheter Based Transducers using the Resolution Integral

Elsevier Editorial System(tm) for Ultrasound in Medicine and Biology

Manuscript Draft

Manuscript Number: UMB-D-18-00032R2

Title: Evaluation of Intravascular Ultrasound Catheter Based Transducers using the Resolution Integral

Article Type: Original Contribution

Keywords: Intravascular Ultrasound, Phantom, Resolution, IVUS, Transducers, Evaluation, Equipment, Resolution Integral, Imaging Performance

Corresponding Author: Mr. Christopher McLeod,

Corresponding Author's Institution: NHS Lothian

First Author: Christopher McLeod

Order of Authors: Christopher McLeod; Carmel M Moran, PhD; Karne A McBride; Stephen D Pye, PhD

Abstract: Intravascular ultrasound (IVUS) catheters are a specialist imaging modality used in the assessment of cardiovascular disease. The ultrasound transducer may either be of single element mechanical or phased array design. Due to their design and operating frequencies (10-45 MHz), evaluation of the imaging performance is not possible with commercially available ultrasound test objects. A modification of an existing test object, the Edinburgh Pipe Phantom (EPP), was carried out to allow measurement of resolution integral (R), depth of field (Lr) and characteristic resolution (Dr) of IVUS catheters. In total seven IVUS catheters, from two manufacturers and of both single element mechanical and phased array design, were tested to provide a measure of performance over different frequencies and technologies. Measurements of R for the tested IVUS catheters ranged from 11.6 to 18.8. The modified EPP therefore allows catheter based ultrasound probes to be evaluated scientifically and their performance to be seen in relation to other similar ultrasound technologies such as preclinical ultrasound and endoscopic ultrasound.

Suggested Reviewers:

Opposed Reviewers:

Title Page

Evaluation of Intravascular Ultrasound Catheter Based Transducers using the Resolution Integral

[1]C McLeod, [2]C M Moran, [1]K A McBride, [1]S D Pye
1. Medical Physics, NHS Lothian, Edinburgh Royal Infirmary, EH16 4SA, UK
2. Centre for Cardiovascular Science, University of Edinburgh, EH16 4TJ, UK
Corresponding author: Christopher McLeod. email:
christopher.mcleod@nhslothian.scot.nhs.uk

Abstract

Intravascular ultrasound (IVUS) catheters are a specialist imaging modality used in the assessment of cardiovascular disease. The ultrasound transducer may either be of single element mechanical or phased array design. Due to their design and operating frequencies (10-45 MHz), evaluation of the imaging performance is not possible with commercially available ultrasound test objects. A modification of an existing test object, the Edinburgh Pipe Phantom (EPP), was carried out to allow measurement of resolution integral (R), depth of field (Lr) and characteristic resolution (Dr) of IVUS catheters. In total seven IVUS catheters, from two manufacturers and of both single element mechanical and phased array design, were tested to provide a measure of performance over different frequencies and technologies. Measurements of R for the tested IVUS catheters ranged from 11.9 to 18.8. The modified EPP therefore allows catheter based ultrasound probes to be evaluated scientifically and their performance to be seen in relation to other similar ultrasound technologies such as preclinical ultrasound and endoscopic ultrasound.

Key Words

Intravascular Ultrasound, Phantom, Resolution, IVUS, Transducers, Evaluation, Equipment, Resolution Integral, Imaging Performance

Introduction

The ever growing and diverse range of applications of diagnostic ultrasound has led to the development of a range of specialised ultrasound transducers. Many of these transducers do not undergo routine performance testing due either to limitations of target location and size in commercially available performance test phantoms or the inability to obtain useful and meaningful results from these phantoms. One such technology is high frequency catheter based ultrasound imaging. This includes: intravascular ultrasound (IVUS), transurethral ultrasound (TUUS) (Ingrama et al. 2003) and intraductal ultrasound (IDUS) catheters (Levy et al. 2002). Despite different clinical applications these transducers share design similarities and are either single element mechanical or phased array micro ultrasound transducers contained within catheters of diameters less than 3mm. Catheter based transducers typically do not have adjustable operating frequencies. Instead different models come at a stated centre frequency appropriate for the anatomy of interest. A range of commercial IDUS and TUUS probes are available between 10 MHz to 30 MHz, while those available for IVUS range from 10 MHz to 45 MHz. Clinically, IVUS is employed to give a 360^{o} view of blood vessel structures for the assessment of cardiovascular disease and stent placement.

The primary focus of test techniques and published guidance on grey-scale imaging to date has been with respect to clinical ultrasound operating at frequencies below 20MHz. These frequencies are typical of those used on clinical radiology and cardiology ultrasound scanners. These test techniques are used for regular quality assurance protocols (Dudley et al. 2014; Hangiandreou et al. 2013; Russell 2010)

and also to assess new technologies and provide a technical justification for equipment purchases (Pye et al. 2011). The non-traditional shape of catheter based transducers and their higher operating frequencies make the testing procedures for the acquisition of meaningful performance data from commercial phantoms difficult to obtain. Previous published work from Hoskins et al. (1994) and Elliott et al. (1996) describes test procedures for assessing the performance of single element mechanical transducers (axial, lateral and out of plane resolution and penetration depth). Both employed high contrast targets; Elliott et al. (1996) used polyester filaments in water to measure resolution via the Rayleigh criteria while Hoskins et al. (1994) used nylon filament in water to measure resolution using the point spread function. Hoskin et al. (1994) also utilised a tissue mimicking material to measure low contrast penetration. Some studies have focused on the variability and reliability of calliper measurements made with both single element mechanical and phased array IVUS transducers. For example, Tardif et al. (2000) demonstrated that both single element mechanical and phased array IVUS probes demonstrated low variability in a variety of measurements within a veterinary/clinical setting. Artefacts unique to IVUS transducers such as non uniform rotational distortion (NURD) have been reported. This non uniform rotation of cable-driven single element mechanical transducers leads to a misregistration of the received image lines (Kimura et al. 1996). The effect has also been assessed in comparison to optical coherence tomography (OCT) (Kawase et al. 2007). When assessing accuracy and/or the extent of NURD artefact, a stent phantom has typically been employed. These are constructed of metal wires in a circular distribution and are analogous to the calliper measurement test objects that will be familiar to many Medical Physics, Biomedical and Clinical Engineering departments. The incorporation of a grey-scale test object

to characterise beam shape and the imaging capabilities of IVUS transducers would complement the current methods for assessing image registration accuracy. The single use nature of IVUS catheters reduces the advantages of a routine testing protocol. Instead a strong technical evidence base would be of benefit as justification of current equipment's capabilities and for equipment evaluation prior to procurement. This is of particular importance as IVUS equipment is routinely integrated into the catheterization laboratory potentially locking the hospital into a single supplier.

The Edinburgh Pipe Phantom (EPP) has previously been used to demonstrate improvements in imaging technology over time and to distinguish transducers suited to particular clinical applications (MacGillivray et al. 2010; Pye & Ellis 2011; Inglis et al. 2014). The EPP contains fluid filled anechoic pipe structures that are of various diameters within an agar-based tissue mimicking material (TMM). Each pipe is imaged to determine the depth range L over which the pipe is visible following the procedure described in MacGillivray et al. (2010). The depth range L is plotted as a function of the inverse of effective pipe diameter α. The effective pipe diameter is taken as the geometric mean of the pipe diameter in the imaging and elevation planes. Plotting L(α) generates a curve that is dependent on the specific transducer’s beam shape (Figure 1). The resolution integral (R) is defined as the area under the curve and also corresponds to the ratio of penetration to lateral resolution (MacGillivray et al. 2010). In addition to the resolution integral, two additional metrics are derived from the L(α) curve: characteristic resolution and depth of field. The depth of field (Lr) defines the axial extent of a region of optimum imaging, analogous to the focal region. The characteristic resolution (Dr) is

representative of the beam width within the depth of field. These three parameters are related by the equation R=Lr/Dr. Generated from one set of measurements, R, Dr & Lr are used to characterise and compare different transducer types and systems. Other test methods often generate large data sets from which it can be difficult to determine the relative strength and weakness of different transducers and systems (Madsen et al. 2000; Thijssen et al. 2007). The EPP employs anechoic targets, the detection of which is critical in many clinical applications. This differs to the high contrast filament methods used for example by Hoskins et al. (1994) and Elliott et al. (1996). The key contribution of the work described here is that measurements obtained from a range of depths using IVUS transducers are combined in a physically meaningful way, folding in the effects of lateral and elevation resolution, speckle, low contrast penetration, scan line density, electrical noise and pixel interpolation. This allows them to be compared both with other IVUS transducers and with other clinical and pre-clinical systems.

Modification of the EPP for high frequencies using small diameter pipe structures as described in Moran et al. (2011a) would be appropriate for IVUS transducers. The acoustic properties of the IEC agar-based TMM used to construct the EPP have been well characterised over a frequency range of 2 to 60 MHz (Rabell et al. 2017; Rajagopal et al. 2014; Sun et al. 2012) making it suitable for use at typical IVUS frequencies. Some modifications to the EPP design were required to make it better suited for use with IVUS transducers. For example the ten anechoic pipe structures within the original EPP have diameters ranging from 0.42 to 7.9 mm which is an appropriate range for probes at frequencies from 1-20 MHz. With IVUS frequencies ranging from 10-45 MHz, smaller pipe diameters were required to adequately test

the resolution limit of these transducers. Similarly the depth of the phantom could be reduced as penetration can be expected to be much less at these high frequencies. Importantly, the ability to be able to hold and support the delicate catheters is a necessary feature of a modified EPP for IVUS imaging. To that end the aim of this study was to design and manufacture a modified EPP and use it for characterising various intravascular ultrasound catheter based transducers.

Methods

Like the original EPP, the modified EPP was an agar based TMM which incorporates anechoic pipes structures set at 50^{o} to the scan surface. These anechoic pipes structures were created from an initial mould using metal rods, wires and monofilament sutures of appropriate diameter traversing a plastic container, into which the TMM mixture was poured and set (Pye et al. 2011, Moran et al. 2011b). Care was taken to ensure that metal wires and sutures were taut across the plastic container, secured and sealed to the exterior of the container to prevent leaking of the TMM before it set. The schematics for this are shown in Figure 2, with ten pipes ranging in diameter from 0.044 mm to 1.5 mm spread across several small TMM blocks (64 x 40 x 20 mm). When the TMM blocks had set, the rods, wires and sutures were removed to leave two pairs of anechoic pipes within each block. The blocks were then removed from the mould casing and small cuts made at the corner or edge of each block to uniquely identify them. The blocks were stored in a water-glycerol mix to allow the pipes to fill with fluid and prevent the TMM from drying out. The pipe diameters were chosen to encompass a range of sizes, from diameters large enough to be imaged down to the low contrast penetration (LCP) depth, to

those too small to be detected by the IVUS catheters. This provided a range of data points covering the performance of any given IVUS catheter.

A plastic container was manufactured to accommodate the scanning of TMM blocks, holding two at a time. Guide channels were cut into the container so that plastic guide blocks could move freely along either side of the TMM blocks. These guide blocks had a channel cut to allow a catheter to pass between them and be held securely above the TMM. Confirmation of pipe patency was obtained by scanning the TMM blocks with a VisualSonics Vevo 770 preclinical scanner using a 30 MHz RMV704 probe. The Vevo 770 allowed 3D scans of the pipes as shown in Figure 3. All pipes down to 0.073 mm diameter were imaged using this scanner to ensure that they were free from manufacturing defects.

Two TMM block groups were created from one batch of TMM. These were labelled block groups A & B and used to perform tests on the seven probe models shown in Table 1. To conduct each experiment the IVUS probe was inserted into a channel cut into the guide blocks fixing it above the TMM blocks and allowing positioning to be done via movement of the guide blocks. An example of this can be seen in Figure 4. With the transducer placed over the top of the pipe to be imaged the operator is free to optimise scanner settings to obtain the best image of the pipe. For the Boston Scientific Opticross probe, four sets of measurements were obtained on both group A and group B. All other probes had two sets of measurements recorded from group A and two from group B. Due to the lower frequency of the Volcano Visions PV.035 10 MHz probe, four sets of additional data points were acquired by imaging the larger pipes within the original EPP (diameters: 1.0 mm, 2.0

mm and 3.0 mm). These data points were combined with data obtained from the 1.5 mm pipe and LCP measurements on the modified EPP, to provide an overall measurement.

Following the method described in MacGillivray et al. (2010), each pipe was scanned with depth and gain optimized so as to image the superficial portion of each pipe, closest to the surface of the catheter. For pipes larger than the beam width the visible portion was seen up to the surface of the TMM. On smaller pipes the superficial portion of the pipe disappeared into the surrounding speckle before reaching the surface of the TMM. The point at which this occurred was dependent on the relation between the pipe diameter and the probe beam width. The images were saved to allow measurements to be made off-line. With the aid of the guides, the catheter was then moved to locate the deepest visible position of each pipe i.e. the portion of pipe that was just distinguishable from the surrounding speckle. The viewing depth and gain were adjusted as necessary, and the images saved for off-line measurement. This process was repeated for the upper and lower portions of each pipe, swapping out the pipe blocks until all the pipes had been imaged. The LCP was determined by measuring the distance from the surface of the TMM down to the deepest speckle identifiable from noise. This was done in real time in a section of TMM where no pipes were visible in the field of view. For the majority of the transducers tested the images could be exported to USB/Disc in DICOM format to allow measurement on a review station. However to obtain images from the Boston Scientific Clearview with Atlantis SR Pro and Pro^2 probes, an 8 bit, 20 MHz image capture card (PicPort, CameraTec AG, Weisslingen, Switzerland) was used. Measurements of the depth range L over which the pipe is visible were obtained by

subtracting the most superficial visible depth from the deepest visible depth (Figure 5). This was carried out using ImageJ (U. S. National Institute of Health, Bethesda, Maryland). If required, images were rotated in ImageJ so that the pipe was visualised below the centre point of the image. A piece of thin card into which a slot had been cut to form a viewing aperture was moved along the length of the pipe to allow the observer to compare the pipe with adjacent speckle and identify the most superficial and deepest depths at which the image of the pipe could be confidently detected from background speckle. The width of the slot size varied with probe frequency and the scaling of the image on the screen and was calculated using the protocol outlined in MacGillivray et al. (2010). For each pipe, measurements were averaged and the visible depth range L of each pipe was calculated. A plot of L versus α was then made (following Figure 1) and Dr, Lr and R were calculated using the method given in MacGillivray et al. (2010). The reported 95% confidence interval for Dr, Lr and R was calculated as the standard error of the sample mean multiplied by a coverage factor based on the number of results obtained for that transducer (UKAS, 2012).

Results

All pipes in the modified EPP were observed to be patent and the surrounding TMM had no visible artefacts caused by solid or gaseous inclusions when assessed on the Vevo 770 scanner. The resolution integral of all the IVUS probes tested using the modified EPP are shown in Table 1 and range from 11.9 to 18.8, Lr and Dr are also shown.

The Atlantis SR Pro and Atlantis SR Pro^2 probes on the Boston Scientific Clearview are both 40 MHz single element mechanical probes and both detected measurable lengths of five different pipe diameters, the smallest of which was 0.19 mm. The Boston Scientific Opticross on the Polaris system was also a 40 MHz single element mechanical probe which imaged all the pipes down to the 0.19 mm pipe. As can been seen from Figure 6, the Atlantis SR Pro and Pro^2 are almost identical in terms of performance given the overlap of the measurement uncertainties. The Opticross imaged less of the length of the 1.5 mm pipe compared to the two Atlantis probes and had a smaller LCP resulting in a smaller Lr compared to the Atlantis probes. The Volcano Revolution Rotational 45 MHz Imaging probe was a single element mechanical probe that performed similarly to the Boston Scientific single element mechanical probes imaging down to the 0.19 mm pipe. The Volcano S5 system also offered three phased array probes to be tested. The Eagle Eye platinum was a phased array design with a stated frequency of 20 MHz; it imaged four pipes the smallest of which was 0.33 mm. The Visions PV .018 with a stated frequency of 20 MHz was also a phased array design and imaged three pipes, the smallest of which was 0.33 mm. The Visions PV.035 10 MHz probe detected only the 1.5 mm pipe in the modified EPP. To provide suitable data points to calculate the resolution integral additional pipes from the original EPP were scanned with the Visions PV.035 probe. Compared to the single element mechanical probes the phased array probes recorded the largest Lr and Dr values.

There was a greater uncertainty in the measurement of the resolution integral for the Atlantis SR Pro and Visions PV0.18; 18.8 ± 13% and 14.2 ± 14% respectively. This occurred from differences in resolution integral measurements made with TMM

block group A and TMM block group B. For the Atlantis SR Pro the resolution integral was consistently higher for group B compared to group A, the Visions PV.018 showed the reverse pattern. In each case group A was scanned first immediately followed by group B. Other transducers showed no difference between the TMM blocks and had 95% confidence interval typically ± 6%.

Discussion

The modified EPP design implemented for the evaluation of IVUS transducers in this study proved to be effective. The size and range of pipes included in the modified EPP design were best suited to testing catheter based transducers with frequencies greater than 20 MHz. As the 10 MHz probe was only able to detect one pipe the phantom could benefit from one or more larger pipes when low frequency (10-30 MHz) catheter transducers such as those used in endoscopy are of interest.

The 10 MHz and 20 MHz phased array IVUS probes have greater depth of field (L_r>5 mm) and larger characteristic resolution (D_r>0.4 mm) as one might expect compared to the 40 MHz and 45 MHz single element mechanical IVUS probes. The Eagle Eye Platinum 20 MHz phased array probe with a D_r of 0.39 mm and L_r of 5.9 mm places it in between the two aforementioned groups. The Atlantis SR Pro and Atlantis SR Pro^2 displayed nearly identical results, evidence perhaps that these are equivalent probes with small design/manufacturing differences.

The higher measurement uncertainty on the Atlantis SR Pro and Visions PV .018 probes is possibly the result of a lack in operator familiarity with the scanners, as

281 they were the first probes to be tested on the respective IVUS scanners, which
282 operate differently from clinical radiology scanners. No drop off in measured image
283 performance of the IVUS catheters occurred as might have been expected from
284 single use devices, although each probe's scanning time totalled up to 8 hours
285 across 2 to 3 days. A 95% confidence interval of ± 6% is higher than the ± 2.6%
286 (MacGillivray et al. 2010) in measured value of R reported for linear and curvilinear
287 probe's using the original EPP, again potentially highlighting the challenges of testing
288 IVUS probes. Due to the design of the guide blocks, the process of scanning the
289 TMM blocks was easier to implement than manual scanning of the IVUS probe on
290 the original EPP. Manual scanning on the original EPP led to the catheters
291 becoming bent as a result of the constant handling and scanning angle.
292
293 In Figure 7, results for the single element mechanical IVUS transducers are
294 displayed alongside results from previous studies that used the EPP method to
295 characterise single element mechanical transducers used in preclinical work (Moran
296 et al. 2011b) and endoscopic ultrasound (Inglis et al. 2014). Given the physical
297 constraints of placing transducers within the body of a catheter it is not surprising to
298 find the magnitude of the resolution integral of the IVUS catheters (range 15-19) to
299 be slightly less but comparable to values for single element preclinical probes (range
300 19-25). A common imaging artefact in IVUS, non uniform rotation distortion (NURD)
301 was observed on single element mechanical catheters. It was most prevalent on the
302 Atlantis SR Pro and Pro^2, and although not always present, it was very noticeable in
303 some instances (Figure 8). Despite efforts to minimise the curvature of the catheter
304 during testing, the impact of the artefact could not be controlled. Due to the

inconsistent nature of this artefact it was difficult to assess the impact on the measurements made.

The results from this study demonstrate that IVUS imaging performance may be characterised using the EPP. While the EPP can be used to track the development of faults in clinical ultrasound scanners, the single use nature of the catheters and higher uncertainty make it unlikely that the technique would be used to detect faults in IVUS systems. The successful use of this phantom with IVUS probes indicates it should also be suitable for testing of Transurethral Ultrasound and Intraductal Ultrasound. Further work is required to broaden knowledge of the imaging performance of these other catheter based ultrasound transducers.

Conclusions

With a lack of published information on the performance testing of catheter based ultrasound transducers it has been shown in this study that modifications to an existing imaging test technique and phantom can be used. The described modification to the design of the Edinburgh Pipe Phantom made it suitable for testing catheter based transducers. Experience with the testing of IVUS transducers on both the modified and original EPP found the new phantom to be easier to use. Values of resolution integral (R), depth of field (Lr) and characteristic resolution (Dr) allowed the probes tested to be evaluated scientifically and their performance to be seen in relation to other similar ultrasound technologies. This will be of particular use to those interested in characterising IVUS equipment as either part of the procurement process or to support research and clinical studies.

Declarations

This research was conducted with support from an Institute of Physics and Engineering in Medicine (IPEM) Innovation and Research Award granted to SDP.

References

Dudley NJ, Gibson NM. Early experience with automated B-mode quality assurance tests, Ultrasound 2014; 22:15-20

Elliott MR, Thrush AJ. Measurement of resolution in intravascular ultrasound images, Physiol Meas 1996; 17(4): 259–265

Hangiandreou NJ, Stekel SF, Tradup DJ, Gorny KR, King DM. Four-year experience with a clinical ultrasound quality control program, Ultrasound Med Biol 2011; 37(8):1350-135

Hoskins PR, McDicken WN. Techniques for the assessment of the imaging characteristics of intravascular ultrasound scanners, Br J Radiol 1994; 67(799): 695-700.

Levy MJ, Vazquez-Sequeiros E, Wiersema MJ. Evaluation of the pancreaticobiliary ductal systems by intraductal US, Gastrointest Endosc 2002; 55(3): 387-408

Inglis S, Janeczko A, Ellis W, Plevris JN, Pye SD. Assessing the imaging capabilities of radial mechanical and electronic echo-endoscopes using the resolution integral, Ultrasound Med Biol 2014; 40(8): 1896–1907

Ingrama MD, Sooriakumaran P, Palfrey E, Montgomery B, Massouh H. Evaluation of the upper urinary tract using transureteric ultrasound a review of the technique and typical imaging appearances, Clin Radiol 2008; 63(9):1026-1034

Kawase Y, Suzuki Y, Ikeno F, Yoneyama R, Hoshino K, Ly HQ, Lau GT, Hayase M, Yeung AC, Hajjar RJ, Jang IK. Comparison of Nonuniform Rotational Distortion Between Mechanical IVUS and OCT using a Phantom Model, Ultrasound Med Biol 2007; 33: 67–73

Kimura BJ, Bhargava V, Palinski W, Russo RJ, DeMaria AN. Distortion of intravascular ultrasound images because of nonuniform angular velocity of mechanical-type transducers, Am Heart J 1996; 132: 328-336

MacGillivray TJ, Ellis W, Pye SD. The resolution integral: visual and computational approaches to characterising ultrasound images. Phys Med Biol 2010; 55: 5067–5088.

Madsen EL. Quality assurance for grey-scale imaging, Ultrasound Med. Biol. 2000; 26(1): S48–50

Moran CM, Pye SD, Ellis W, Janeczko A, Morris KD, McNeilly AS, Fraser HM. A comparison of the imaging performance of high resolution ultrasound scanners for preclinical imaging, Ultrasound Med Biol 2011a; 37(3-2): 493–501

Moran CM, Ellis W, Janeczko A, Bell D, Pye SD. The Edinburgh Pipe Phantom: characterising ultrasound scanners beyond 50 MHz, J Phys Conf Ser 2011b; 279: 1 - 7

Rabell AM, Browne JE, Pye SD, Anderson TA, Moran CM. Broadband acoustic measurement of an agar-based tissue-mimicking-material: a longitudinal study, Ultrasound Med Biol 2017; 43: 1494-1505

Pye SD, Ellis W. The resolution integral as a metric of performance for diagnostic grey-scale imaging, J Phys Conf Ser 2011; 279: 012009.

UKAS. M3003: The expression of uncertainty and confidence in measurement. Edition 3. Feltham, United Kingdom: UKAS, 2012. Appendix B; 28-30

Rajagopal S, Sadhoo N, Zeqiri B. Reference characterisation of sound speed and attenuation of the IEC agar-based tissue-mimicking material up to a frequency of 60 MHz. Ultrasound Med Biol 2015; 41: 317–333.

Russell S, ed. Institute of Physics and Engineering in Medicine Report 102: Quality Assurance of Ultrasound Imaging Systems 2010; York, UK, IPEM

Sun C, Pye S, Browne JE, Janeczko A, Ellis B, Butler MB, Sboros V, Thomson AJ, Brewin MP, Earnshaw CH, Moran CM. The Speed of Sound and Attenuation of an IEC Agar-Based Tissue-Mimicking Material for High Frequency Ultrasound Applications, Ultrasound Med Biol 2012; 38(7): 1262-1270

Tardif JC, Bertrand OF, Mongrain R, Lespérance J, Grégoire J, Paiement P, Bonan R. Reliability of mechanical and phased-array designs for serial intravascular ultrasound examinations, The Int J of Card Imaging 2000; 16: 365-375

Thijssen JM, Weijers G, de Korte CL. Objective performance testing and quality assurance of medical ultrasound equipment. Ultrasound Med Biol 2007; 33: 460–471

Figures

Figure 1. a) Schematic diagram of L against α for the ultrasound beam generated by an IVUS catheter shown in image b) which illustrates how depth of field Lr and characteristic resolution Dr are defined. The plot of L vs α for the IVUS catheter extends from the low contrast penetration L_0 on the y-axis to $1/D_0$ on the x-axis, where D_0 is the minimum beam width. The area under the curve $L_0 - 1/D_0$ is R. Lr and 1/Dr are the coordinates of O`, the vertex of a rectangle with area R and in which the diagonal OO` bisects the area under the curve $L_0 - 1/D_0$. Thus R=Lr/Dr. Lr and Dr can also be considered as the characteristics of a perfectly collimated ultrasound beam with low contrast penetration Lr and beam width Dr.

Figure 2. a) Rectangular plastic containers act as moulds for the Tissue Mimicking Material (TMM) blocks. The different diameter pipes and sutures were threaded through and held in place with sealant. b) The diameter of each pipe and the block of TMM in which it was located. Each block contained 4 pipes, two of each size. An image of the resulting anechoic pipe structure is shown in a).

Figure 3. 3D scans were obtained for all pipes except the 0.044 mm using a RMV704 probe from a VisualSonics Vevo 770 preclinical ultrasound scanner. This particular pipe shown is 0.33 mm in diameter. The RMV704 probe has a 30 MHz centre-frequency making it suitable for imaging such small targets. The 3D scans provided confidence that were no pockets of gas and that the pipes were patent.

Figure 4. Set up of the IVUS phantom: two TMM blocks, each with anechoic pipe structures, can be held within the Perspex container. The container also houses the

Perspex guide blocks that allow the catheter to be slotted through a channel cut into them so that the catheter is suspended just above the surface of the TMM. Via movement of the guide blocks the catheter can be positioned over the pipe to be imaged and the length of pipe which is distinguishable from background speckle can be measured. This set up places minimal strain on the catheter and allows the operator to adjust imaging settings as required to optimise the image.

Figure 5. Measurement of (a) the superficial visible section of pipe, and b) the deepest visible section of pipe. The depth range L over which the pipe is visible is given by d2 - d1 = 3.7 mm

Figure 6. Graph of depth of field (Lr) versus characteristic resolution (Dr) showing the IVUS results for both single element mechanical and phased array transducers. Error bars show the 95% confidence interval for the Lr and Dr measurements made on each transducer.

Figure 7. A depth of field (Lr) versus characteristic resolution (Dr) plot; shown in black squares are the IVUS single element mechanical transducer results obtained from the modified EPP. Results for preclinical single element mechanical transducers are shown as reported by Moran et al. (2011). Single element mechanical endoscopic ultrasound probes reported by Inglis et al. (2014) are also shown.

Figure 8. Example of the Non Uniform Rotation Distortion (NURD) artefact. a) 1.5 mm pipe imaged with the scan surface horizontal. b) From the same probe an

image of the 0.23 mm pipe. In this image the scan surface has become distorted and appears to slope away from the transducer. This artefact can vary in severity and was seen on the single element mechanical catheters, the example shown is the Atlantis SR Pro. There is also a mirror image and shadowing artefact in the upper half of the image due to reflection from the surface of the TMM fluid.

Tables

Manu.	Scanner	Probe	Transducer Type	Nominal Centre Freq. (MHz)	R	Lr (mm)	Dr (mm)
Boston Sci.	Clearview	Atlantis SR Pro	M	40	**18.8**	**4.91**	**0.26**
Boston Sci.	Clearview	Atlantis SR Pro^2	M	40	**17.2**	**4.88**	**0.28**
Volcano	S5	Eagle Eye platinum	PA	20	**15.3**	**5.94**	**0.39**
Volcano	S5	Revolution Rotational Imaging	M	45	**14.7**	**4.44**	**0.30**
Boston Sci.	iLab	Opticross	M	40	**14.5**	**3.84**	**0.27**
Volcano	S5	Visions PV .018	PA	20	**14.2**	**5.95**	**0.44**
Volcano	S5	Visions PV .035	PA	10	**11.6**	**14.0**	**1.21**

Table 1. The resolution integral (R), characteristic resolution (Dr) and depth of field (Lr). Transducer type noted as M=Single element mechanical, PA=Phased Array.

Figure 1

Click here to download high resolution image

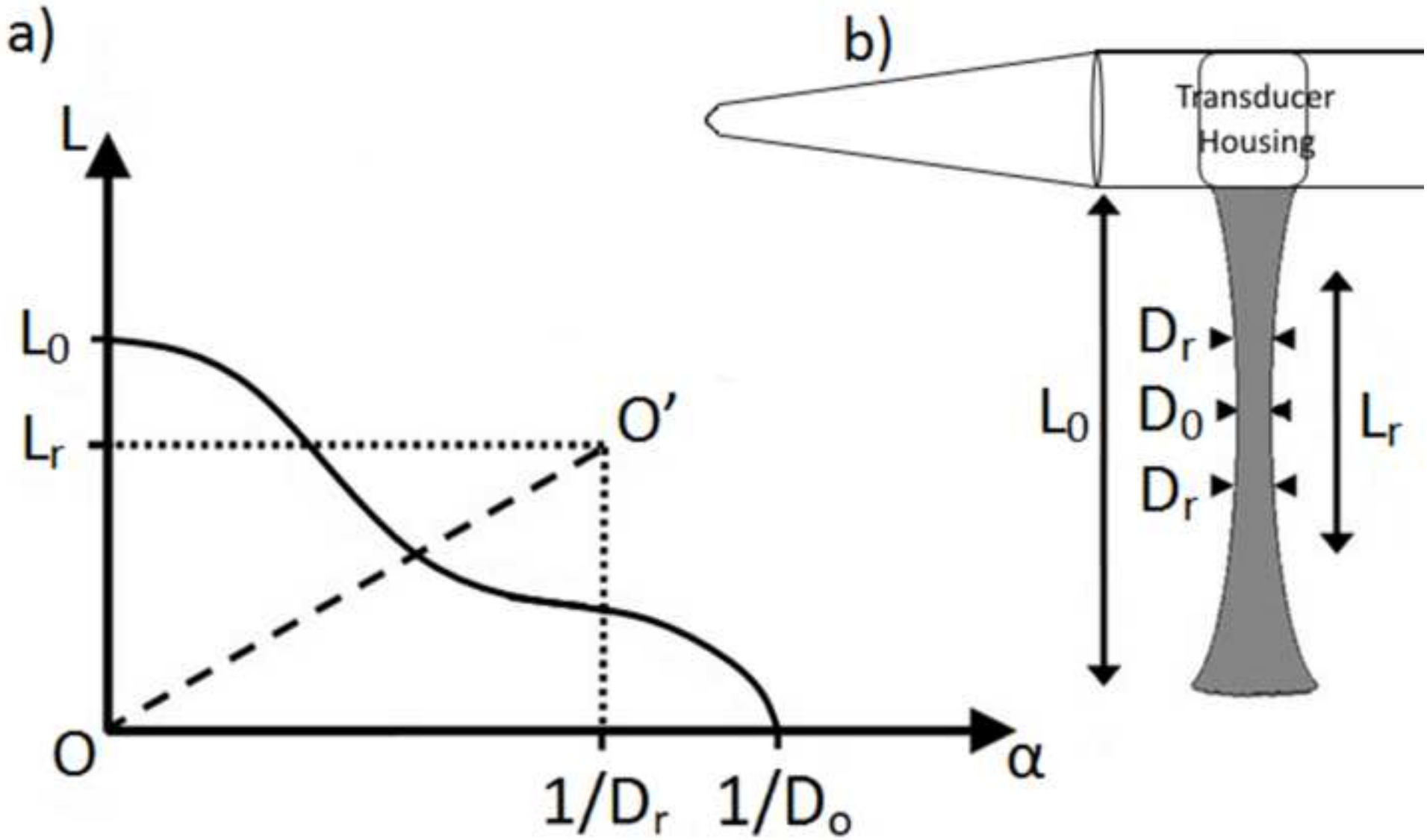

Figure 2

Click here to download high resolution image

a)

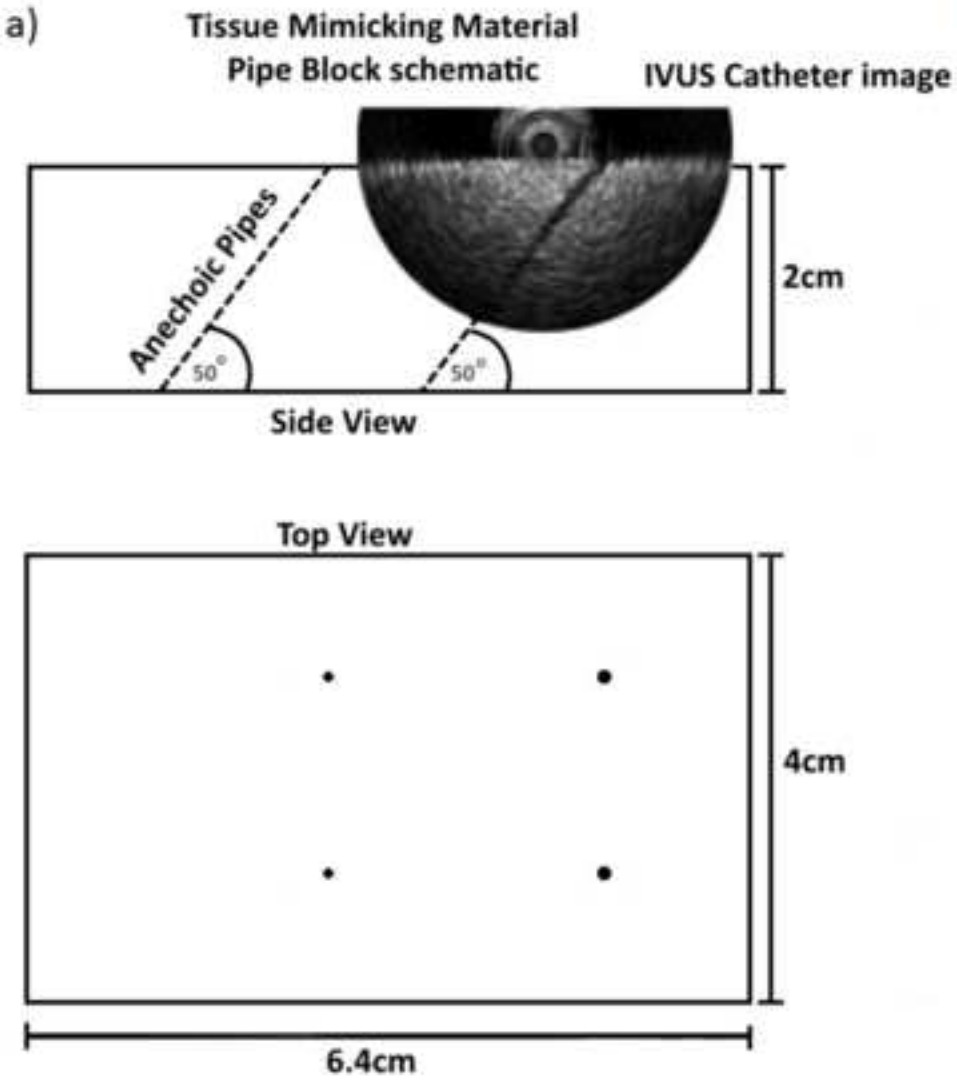

b)

Modified Edinburgh Pipe Phantom (IVUS Phantom)			Original Edinburgh Pipe Phantom
TMM Block	Mould Material	Diameter (mm)	Diameter (mm)
1	Metal Rod	1.5	7.9
1	Metal Rod	0.55	6.0
2	Metal Rod	0.33	4.0
2	Metal Rod	0.23	3.0
3	Monofilament Suture	0.19	2.0
3	Monofilament Suture	0.14	1.5
4	Metal Wire	0.11	1.0
4	Monofilament Suture	0.094	0.72
5	Monofilament Suture	0.073	0.55
5	Metal Wire	0.044	0.42

Figure 3

Click here to download high resolution image

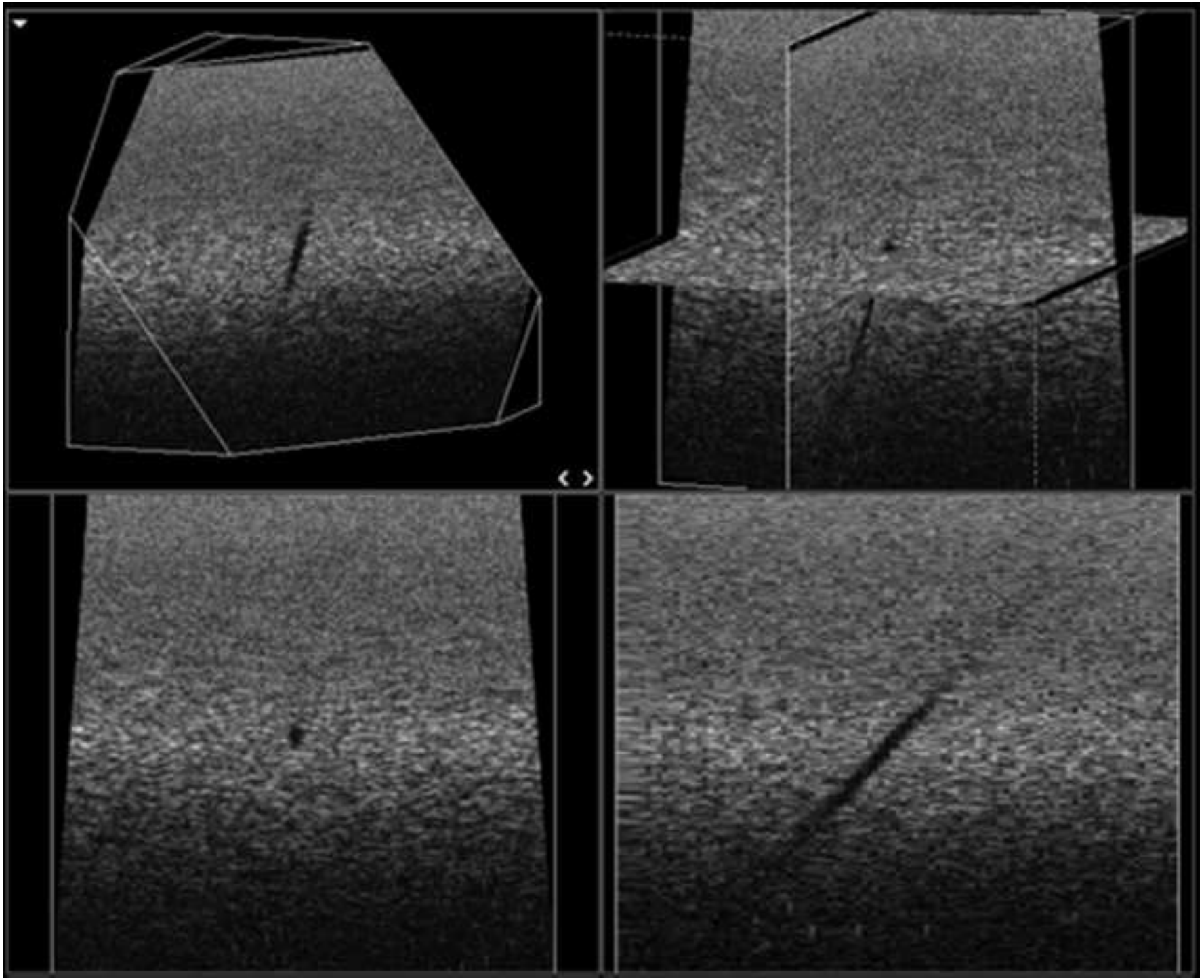

Figure 4

Click here to download high resolution image

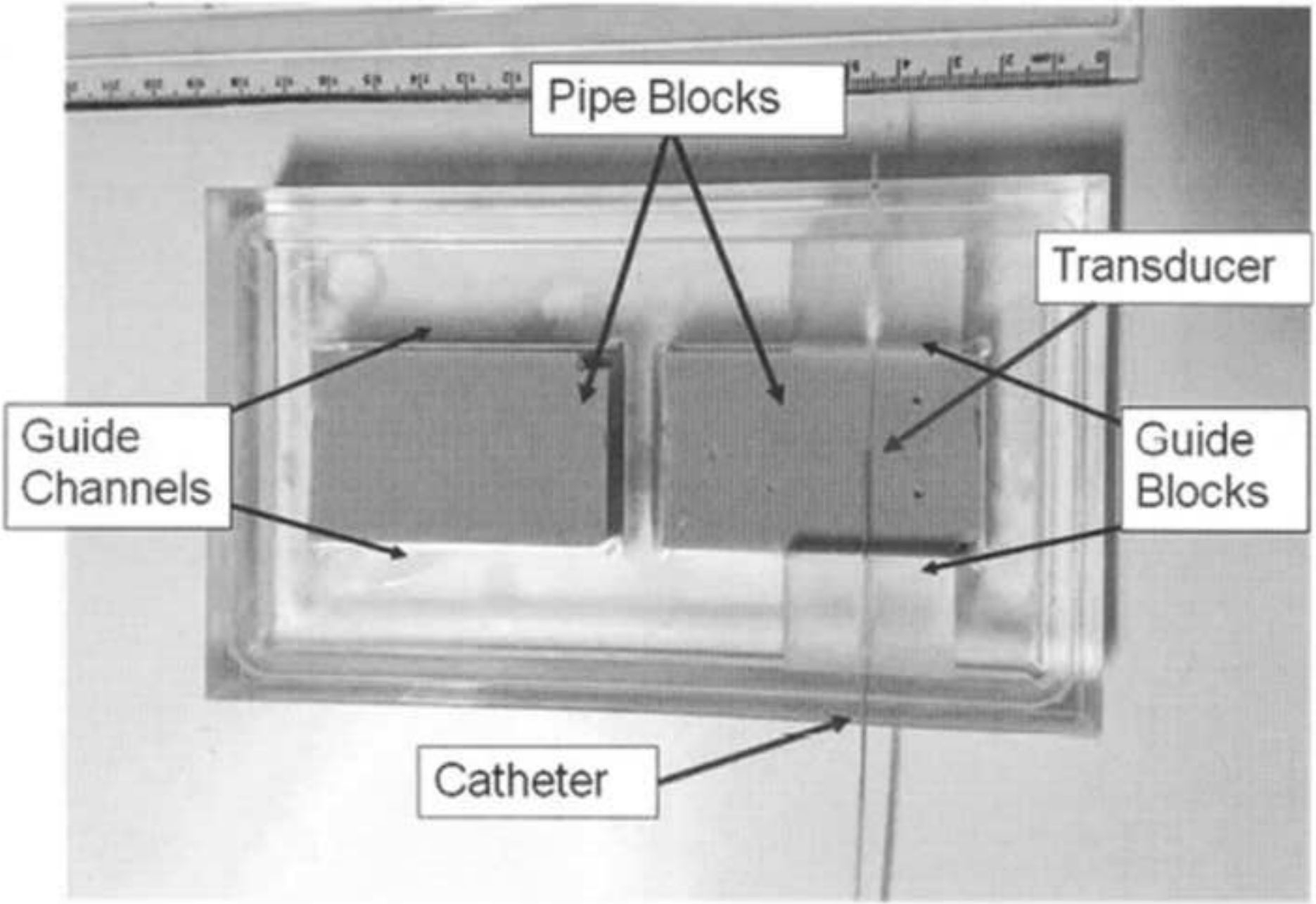

Figure 5

Click here to download high resolution image

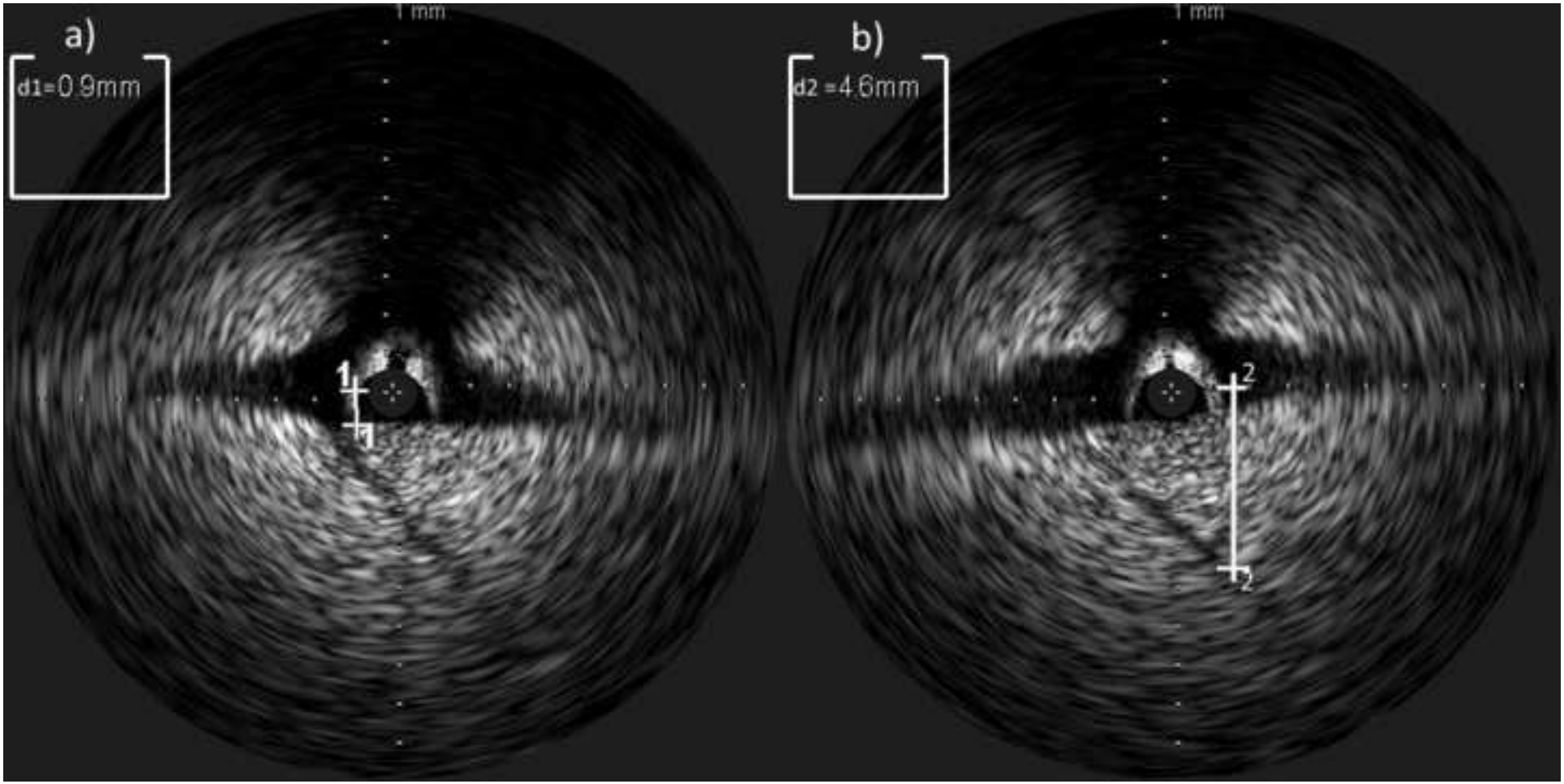

Figure 6

Click here to download high resolution image

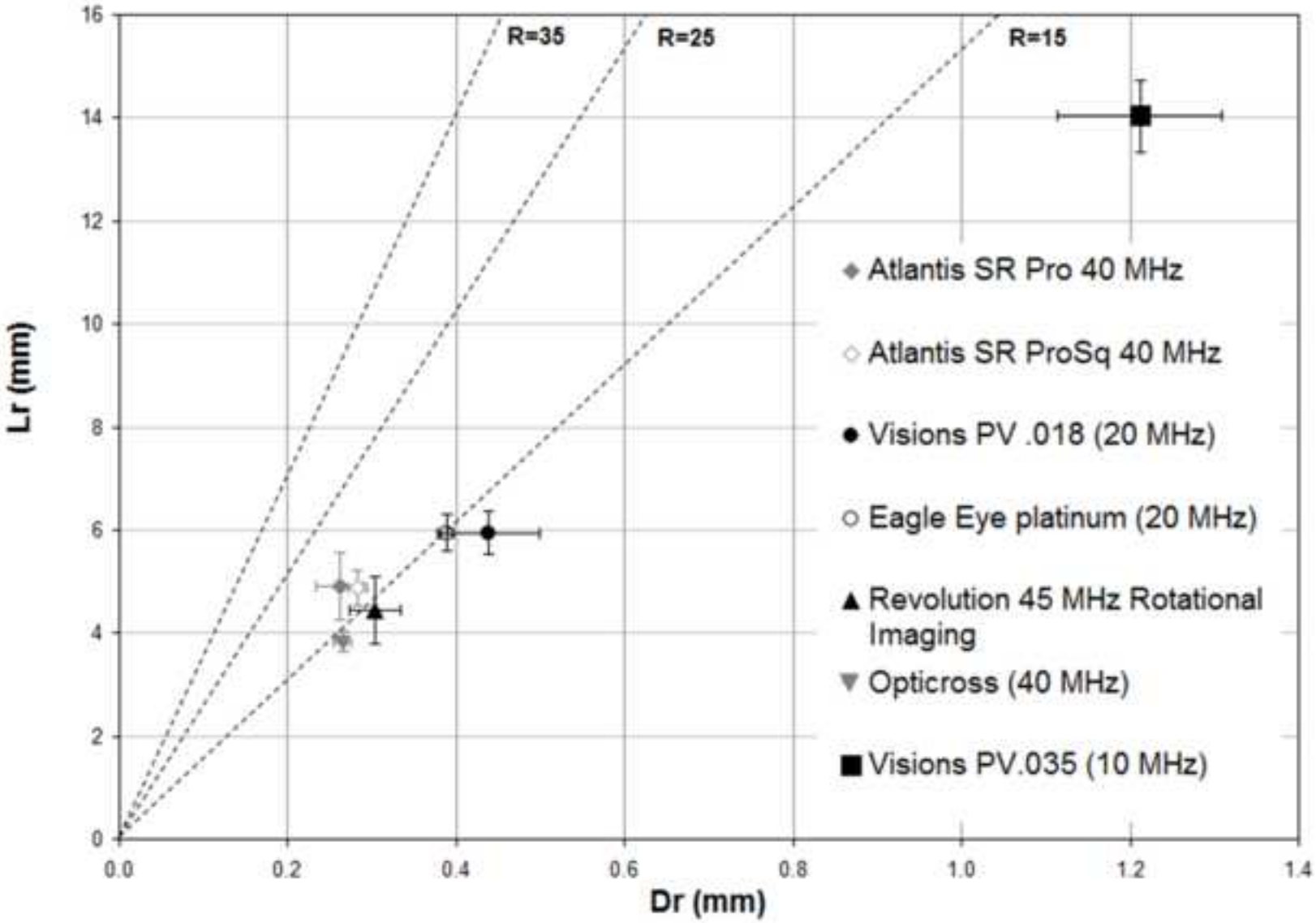

Figure 7

Click here to download high resolution image

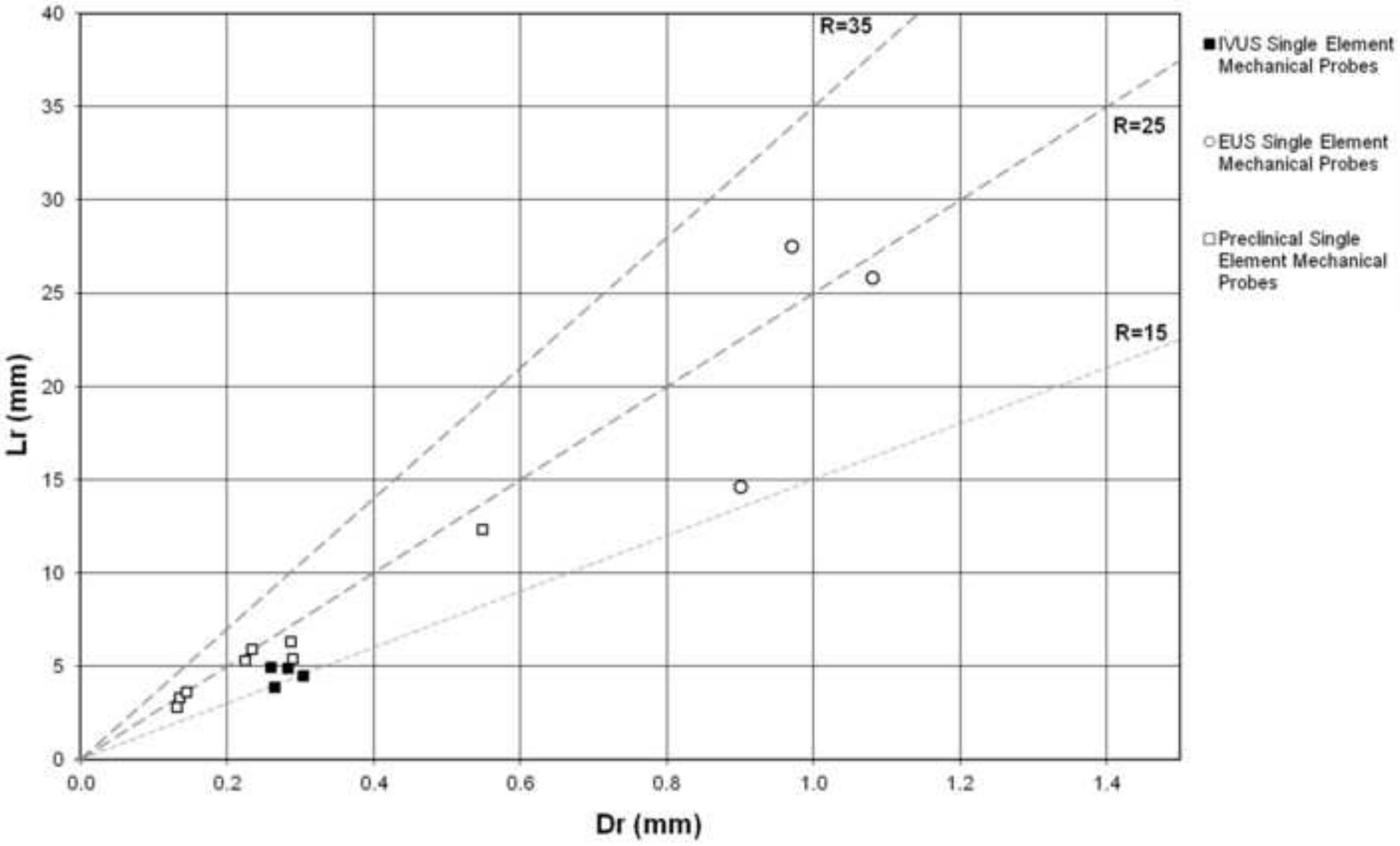

Figure 8

Click here to download high resolution image